

Probing Black Holes and Relativistic Stars with Gravitational Waves

Kip S. Thorne

California Institute of Technology, Pasadena, CA 91125 USA

Abstract

In the coming decade, gravitational waves will convert the study of general relativistic aspects of black holes and stars from a largely theoretical enterprise to a highly interactive, observational/theoretical one. For example, gravitational-wave observations should enable us to observationally map the spacetime geometries around quiescent black holes, study quantitatively the highly nonlinear vibrations of curved spacetime in black-hole collisions, probe the structures of neutron stars and their equation of state, search for exotic types of general relativistic objects such as boson stars, soliton stars, and naked singularities, and probe aspects of general relativity that have never yet been seen such as the gravitational fields of gravitons and the influence of gravitational-wave tails on radiation reaction.

1 Introduction

Subrahmanyan Chandrasekhar and I entered the field of relativistic astrophysics at the same time, in the early 1960s—I as a green graduate student at Princeton; Chandra as an established and famous researcher at the University of Chicago. Over the decades of the 60's, 70's and 80's, and into the 90's, Chandra, I, and our friends and colleagues had the great pleasure of exploring general relativity's predictions about the properties of black holes and relativistic stars. Throughout these explorations Chandra was an inspiration for us all.

When we began, there was no observational evidence that black holes or relativistic stars exist in the Universe, much less that they play important roles. However, in parallel with our theoretical studies, astronomers discovered pulsars and quickly deduced they are spinning neutron stars in which relativistic effects should be strong; astronomers also discovered quasars, and gradually, over three decades' time, came to understand that they are powered by supermassive black holes; astronomers discovered compact X-ray sources and quickly deduced they are binary systems in which gas accretes from a normal star onto a stellar-mass black-hole companion or neutron-star companion; and astronomers discovered gamma ray bursts, and after nearly three decades of puzzlement, have concluded they are probably produced by the final merger of a neutron-star /neutron-star binary or a neutron-star / black-hole binary.

Despite this growing richness of astrophysical phenomena in which black holes and neutron stars play major roles, those of us who use general relativity to predict the properties of these objects have been frustrated: in the rich astronomical data there as yet is little evidence for the holes' and stars' spacetime warpage, which is so central to our theoretical studies. If we had to rely solely on observations and not at all on theory, we could still argue, in 1997, that a black hole is a flat-spacetime, Newtonian phenomenon and neutron stars are un-influenced by general relativistic effects.

Why this frustration? Perhaps because spacetime warpage cannot, itself, produce the only kinds of radiation that astronomers now have at their disposal: electromagnetic waves, neutrinos,

and cosmic rays. To explore spacetime warpage in detail may well require using, instead, the only kind of radiation that such warpage can produce: radiation made of spacetime warpage—gravitational waves.

In this article, I shall describe the prospects for using gravitational waves to probe the warpage of spacetime around black holes and relativistic stars, and to search for new types of general relativistic objects, for which there as yet is no observational evidence. And I shall describe how the challenge of developing data analysis algorithms for gravitational-wave detectors is already driving the theory of black holes and relativistic stars just as hard as the theory is driving the wave-detection efforts. Already, several years before the full-scale detectors go into operation, the challenge of transforming general relativistic astrophysics into an observational science has transformed the nature of our theoretical enterprise. At last, after 35 years of only weak coupling to observation, those of us studying general relativistic aspects of black holes and stars have become tightly coupled to the observational/experimental enterprise.

2 Gravitational Waves

A gravitational wave is a ripple of warpage (curvature) in the “fabric” of spacetime. According to general relativity, gravitational waves are produced by the dynamical spacetime warpage of distant astrophysical systems, and they travel outward from their sources and through the Universe at the speed of light, becoming very weak by the time they reach the Earth. Einstein discovered gravitational waves as a prediction of his general relativity theory in 1916, but only in the late 1950s did the technology of high-precision measurement become good enough to justify an effort to construct detectors for the waves.

Gravitational-wave detectors and detection techniques have now been under development for nearly 40 years, building on foundations laid by Joseph Weber [1], Rainer Weiss [2], and others. These efforts have led to promising sensitivities in four frequency bands, and theoretical studies have identified plausible sources in each band:

- The Extremely Low Frequency Band (ELF), 10^{-15} to 10^{-18} Hz, in which the measured anisotropy of the cosmic microwave background radiation places strong limits on gravitational wave strengths—and may, in fact, have detected waves [3, 4]. The only waves expected in this band are relics of the big bang, a subject beyond the scope of this article. (For some details and references see [3, 4, 5] and references cited therein.)
- The Very Low Frequency Band (VLF), 10^{-7} to 10^{-9} Hz, in which Joseph Taylor and others have achieved remarkable gravity-wave sensitivities by the timing of millisecond pulsars [6]. The only expected strong sources in this band are processes in the very early universe—the big bang, phase transitions of the vacuum states of quantum fields, and vibrating or colliding defects in the structure of spacetime, such as monopoles, cosmic strings, domain walls, textures, and combinations thereof [7, 8, 9, 10]. These sources are also beyond the scope of this article.
- The Low-Frequency Band (LF), 10^{-4} to 1 Hz, in which will operate the Laser Interferometer Space Antenna, LISA; see Sec. 3.4 below. This is the band of massive black holes ($M \sim 1000$ to $10^8 M_\odot$) in the distant universe, and of other hypothetical massive exotic objects (naked singularities, soliton stars), as well as of binary stars (ordinary, white dwarf, neutron star, and black hole) in our galaxy. Early universe processes should also have produced waves at these frequencies, as in the ELF and VLF bands.

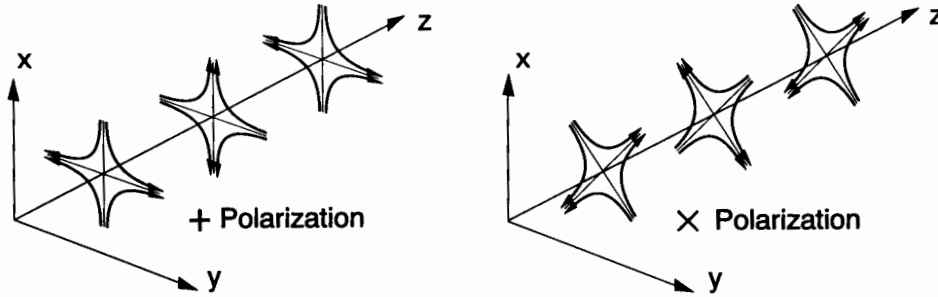


Figure 1: The lines of force associated with the two polarizations of a gravitational wave. (From Ref. [12].)

- The High-Frequency Band (HF), 1 to 10^4 Hz, in which operate earth-based gravitational-wave detectors such as LIGO; see Secs. 3.1–3.3 below. This is the band of stellar-mass black holes ($M \sim 1$ to $1000 M_\odot$) and of other conceivable stellar-mass exotic objects (naked singularities and boson stars) in the distant universe, as well as of supernovae, pulsars, and coalescing and colliding neutron stars. Early universe processes should also have produced waves at these frequencies, as in the ELF, VLF, and LF bands.

In this article I shall focus on the HF and LF bands, because these are the ones in which we can expect to study black holes and relativistic stars.

One aspect of a gravitational wave’s spacetime warpage—the only aspect relevant to earth-based detectors—is an oscillatory “stretching and squeezing” of space. This stretch and squeeze is described, in general relativity theory, by two dimensionless gravitational wave fields h_+ and h_\times (the “strains of space”) that are associated with the wave’s two linear polarizations, conventionally called “plus” (+) and “cross” (\times). The fields h_+ and h_\times , technically speaking, are the double time integrals of space-time-space-time components of the Riemann curvature tensor; and they propagate through spacetime at the speed of light. The inertia of any small piece of an object tries to keep it at rest in, or moving at constant speed through, the piece of space in which it resides; so as h_+ and h_\times stretch and squeeze space, inertia stretches and squeezes objects that reside in that space. This stretch and squeeze is analogous to the tidal gravitational stretch and squeeze exerted on the Earth by the Moon, and thus the associated gravitational-wave force is referred to as a “tidal” force.

If an object is small compared to the waves’ wavelength (as is the case for ground-based detectors), then relative to the object’s center, the waves exert tidal forces with the quadrupolar patterns shown in Fig. 1. The names “plus” and “cross” are derived from the orientations of the axes that characterize the force patterns [11].

The strengths of the waves from a gravitational-wave source can be estimated using the “Newtonian/quadrupole” approximation to the Einstein field equations. This approximation says that $h \simeq (G/c^4)\ddot{Q}/r$, where \ddot{Q} is the second time derivative of the source’s quadrupole moment, r is the distance of the source from Earth (and G and c are Newton’s gravitation constant and the speed of light). The strongest sources will be highly nonspherical and thus will have $Q \simeq ML^2$, where M is their mass and L their size, and correspondingly will have $\ddot{Q} \simeq 2Mv^2 \simeq 4E_{\text{kin}}^{\text{ns}}$, where v is their internal velocity and $E_{\text{kin}}^{\text{ns}}$ is the nonspherical part of their internal kinetic energy. This provides us with the estimate

$$h \sim \frac{1}{c^2} \frac{4G(E_{\text{kin}}^{\text{ns}}/c^2)}{r}; \quad (1)$$

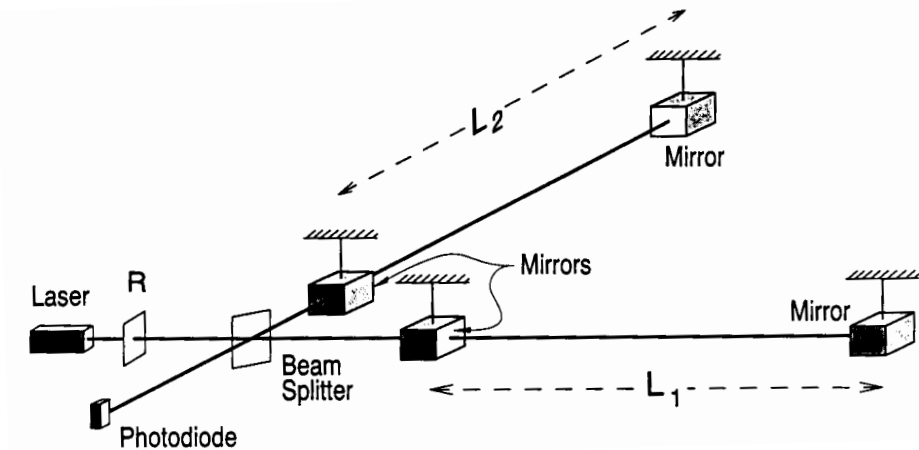


Figure 2: Schematic diagram of a laser interferometer gravitational wave detector. (From Ref. [12].)

i.e., h is about 4 times the gravitational potential produced at Earth by the mass-equivalent of the source's nonspherical, internal kinetic energy—made dimensionless by dividing by c^2 . Thus, in order to radiate strongly, the source must have a very large, nonspherical, internal kinetic energy.

The best known way to achieve a huge internal kinetic energy is via gravity; and by energy conservation (or the virial theorem), any gravitationally-induced kinetic energy must be of order the source's gravitational potential energy. A huge potential energy, in turn, requires that the source be very compact, not much larger than its own gravitational radius. Thus, the strongest gravity-wave sources must be highly compact, dynamical concentrations of large amounts of mass (e.g., colliding and coalescing black holes and neutron stars).

Such sources cannot remain highly dynamical for long; their motions will be stopped by energy loss to gravitational waves and/or the formation of an all-encompassing black hole. Thus, the strongest sources should be transient. Moreover, they should be very rare—so rare that to see a reasonable event rate will require reaching out through a substantial fraction of the Universe. Thus, just as the strongest radio waves arriving at Earth tend to be extragalactic, so also the strongest gravitational waves are likely to be extragalactic.

For highly compact, dynamical objects that radiate in the high-frequency band, e.g. colliding and coalescing neutron stars and stellar-mass black holes, the internal, nonspherical kinetic energy $E_{\text{kin}}^{\text{ns}}/c^2$ is of order the mass of the Sun; and, correspondingly, Eq. (1) gives $h \sim 10^{-22}$ for such sources at the Hubble distance (3000 Mpc, i.e., 10^{10} light years); $h \sim 10^{-21}$ at 200 Mpc (a best-guess distance for several neutron-star coalescences per year; see Section 6.2), $h \sim 10^{-20}$ at the Virgo cluster of galaxies (15 Mpc); and $h \sim 10^{-17}$ in the outer reaches of our own Milky Way galaxy (20 kpc). These numbers set the scale of sensitivities that ground-based interferometers seek to achieve: $h \sim 10^{-21}$ to 10^{-22} .

3 Gravitational Wave Detectors in the High and Low Frequency Bands

3.1 Ground-Based Laser Interferometers

The most promising and versatile type of gravitational-wave detector in the high-frequency band, 1 to 10^4 Hz, is a laser interferometer gravitational wave detector (“interferometer” for short). Such an interferometer consists of four mirror-endowed masses that hang from vibration-isolated supports as shown in Fig. 2, and the indicated optical system for monitoring the separations between the masses [11, 12]. Two masses are near each other, at the corner of an “L”, and one mass is at the end of each of the L’s long arms. The arm lengths are nearly equal, $L_1 \simeq L_2 = L$. When a gravitational wave, with frequencies high compared to the masses’ ~ 1 Hz pendulum frequency, passes through the detector, it pushes the masses back and forth relative to each other as though they were free from their suspension wires, thereby changing the arm-length difference, $\Delta L \equiv L_1 - L_2$. That change is monitored by laser interferometry in such a way that the variations in the output of the photodiode (the interferometer’s output) are directly proportional to $\Delta L(t)$.

If the waves are coming from overhead or underfoot and the axes of the + polarization coincide with the arms’ directions, then it is the waves’ + polarization that drives the masses, and the detector’s strain $\Delta L(t)/L$ is equal to the waves’ strain of space $h_+(t)$. More generally, the interferometer’s output is a linear combination of the two wave fields:

$$\frac{\Delta L(t)}{L} = F_+ h_+(t) + F_\times h_\times(t) \equiv h(t) . \quad (2)$$

The coefficients F_+ and F_\times are of order unity and depend in a quadrupolar manner on the direction to the source and the orientation of the detector [11]. The combination $h(t)$ of the two h ’s is called the gravitational-wave strain that acts on the detector; and the time evolutions of $h(t)$, $h_+(t)$, and $h_\times(t)$ are sometimes called *waveforms*.

When one examines the technology of laser interferometry, one sees good prospects to achieve measurement accuracies $\Delta L \sim 10^{-16}$ cm (1/1000 the diameter of the nucleus of an atom)—and $\Delta L = 8 \times 10^{-16}$ has actually been achieved in a prototype interferometer at Caltech [13]. With $\Delta L \sim 10^{-16}$ cm, an interferometer must have an arm length $L = \Delta L/h \sim 1$ to 10 km in order to achieve the desired wave sensitivities, 10^{-21} to 10^{-22} . This sets the scale of the interferometers that are now under construction.

3.2 LIGO, VIRGO, and the International Network of Gravitational Wave Detectors

Interferometers are plagued by non-Gaussian noise, e.g. due to sudden strain releases in the wires that suspend the masses. This noise prevents a single interferometer, by itself, from detecting with confidence short-duration gravitational-wave bursts (though it may be possible for a single interferometer to search for the periodic waves from known pulsars). The non-Gaussian noise can be removed by cross correlating two, or preferably three or more, interferometers that are networked together at widely separated sites.

The technology and techniques for such interferometers have been under development for 25 years, and plans for km-scale interferometers have been developed over the past 15 years. An international network consisting of three km-scale interferometers at three widely separated sites is now under construction. It includes two sites of the American LIGO Project (“Laser Interferometer Gravitational Wave Observatory”) [12], and one site of the French/Italian VIRGO Project (named after the Virgo cluster of galaxies) [14].

LIGO will consist of two vacuum facilities with 4-kilometer-long arms, one in Hanford, Washington (in the northwestern United States) and the other in Livingston, Louisiana (in the southeastern United States). These facilities are designed to house many successive generations of interferometers without the necessity of any major facilities upgrade; and after a planned future expansion, they will be able to house several interferometers at once, each with a different optical configuration optimized for a different type of wave (e.g., broad-band burst, or narrow-band periodic wave, or stochastic wave).

The LIGO facilities are being constructed by a team of about 80 physicists and engineers at Caltech and MIT, led by Barry Barish (the PI), Gary Sanders (the Project Manager), Albert Lazzarini, Rai Weiss, Stan Whitcomb, and Robbie Vogt (who directed the project during the pre-construction phase). This Caltech/MIT team, together with researchers from several other universities, is developing LIGO's first interferometers and their data analysis system. Other research groups from many universities are contributing to R&D for *enhancements* of the first interferometers, or are computing theoretical waveforms for use in data analysis, or are developing data analysis techniques for future interferometers. These groups are linked together in a *LIGO Scientific Collaboration* and by an organization called the *LIGO Research Community*. For further details, see the LIGO World Wide Web Site, <http://www.ligo.caltech.edu/>.

The VIRGO Project is building one vacuum facility in Pisa, Italy, with 3-kilometer-long arms. This facility and its first interferometers are a collaboration of more than a hundred physicists and engineers at the INFN (Frascati, Napoli, Perugia, Pisa), LAL (Orsay), LAPP (Annecy), LOA (Palaiseau), IPN (Lyon), ESPCI (Paris), and the University of Illinois (Urbana), under the leadership of Alain Brillet and Adalberto Giazotto.

The LIGO and VIRGO facilities are scheduled for completion at the end of the 1990's, and their first gravitational-wave searches will be performed in 2001 or 2002. Figure 3 shows the design sensitivities for LIGO's *first interferometers* (ca. 2001) [12] and for *enhanced versions* of those interferometers (which are expected to be operating five years or so later) [15], along with a benchmark sensitivity goal for subsequent, more *advanced interferometers* [12, 15].

For each type of interferometer, the quantity shown is the “sensitivity to bursts” that come from a random direction, $h_{\text{SB}}(f)$ [12]. This h_{SB} is about 5 times worse than the rms noise level in a bandwidth $\Delta f \simeq f$ for waves with a random direction and polarization, and about $5\sqrt{5} \simeq 11$ times worse than the rms noise level h_{rms} for optimally directed and polarized waves. (In much of the literature, the quantity plotted is $h_{\text{rms}} \simeq h_{\text{SB}}/11$.) Along the right-hand branch of each sensitivity curve (above 100 or 200 Hz), the interferometer's dominant noise is due to photon counting statistics (“shot noise”); along the middle branch (10 or 30 Hz to 100 to 200 Hz), the dominant noise is random fluctuations of thermal energy in the test masses and their suspensions; along the steep left-hand branch, the dominant noise is seismic vibrations creeping through the interferometers' seismic isolation system.

The interferometer sensitivity h_{SB} is to be compared with the “characteristic amplitude” $h_c(f) = h\sqrt{n}$ of the waves from a source; here h is the waves' amplitude when they have frequency f , and n is the number of cycles the waves spend in a bandwidth $\Delta f \simeq f$ near frequency f [11, 12]. Any source with $h_c > h_{\text{SB}}$ should be detectable with high confidence, even if it arrives only once per year.

Figure 3 shows the estimated or computed characteristic amplitudes h_c for several sources that will be discussed in detail later in this article. Among these sources are binary systems made of $1.4M_\odot$ neutron stars (“NS”) and binaries made of 10, 25, and $30 M_\odot$ black holes (“BH”), which spiral together and collide under the driving force of gravitational radiation reaction. As the bodies spiral inward, their waves sweep upward in frequency (rightward across the figure

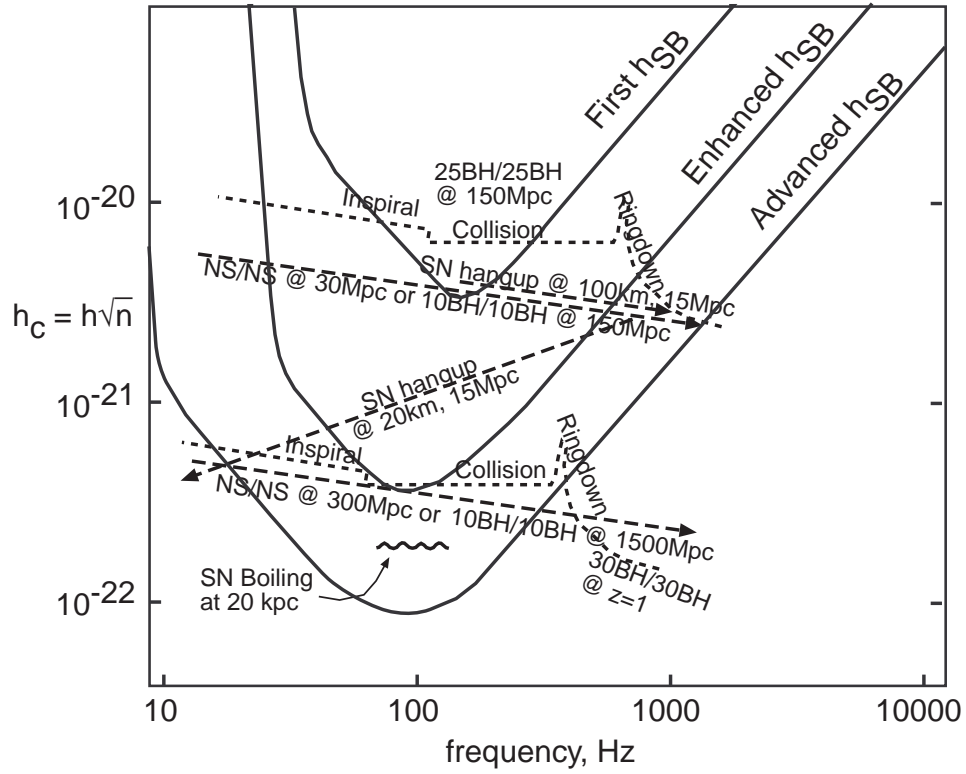


Figure 3: LIGO's projected broad-band noise sensitivity to bursts h_{SB} (Refs. [12, 15]) compared with the characteristic amplitudes h_c of the waves from several hypothesized sources. The signal to noise ratios are $\sqrt{2}$ higher than in Ref. [12] because of a factor 2 error in Eq. (29) of Ref. [11].

along the dashed lines). From the figure we see that LIGO’s first interferometers should be able to detect waves from the inspiral of a NS/NS binary out to a distance of 30Mpc (90 million light years) and from the final collision and merger of a $25M_{\odot}/25M_{\odot}$ BH/BH binary out to about 300Mpc. Comparison with estimated event rates (Secs. 6.2 and 7.2 below) suggests, with considerable confidence, that the first wave detections will be achieved by the time the enhanced sensitivity is reached and possibly as soon as the first-interferometers’ searches.

LIGO alone, with its two sites which have parallel arms, will be able to detect an incoming gravitational wave, measure one of its two waveforms, and (from the time delay between the two sites) locate its source to within a $\sim 1^{\circ}$ wide annulus on the sky. LIGO and VIRGO together, operating as a *coordinated international network*, will be able to locate the source (via time delays plus the interferometers’ beam patterns) to within a 2-dimensional error box with size between several tens of arcminutes and several degrees, depending on the source direction and on the amount of high-frequency structure in the waveforms. They will also be able to monitor both waveforms $h_{+}(t)$ and $h_{\times}(t)$ (except for frequency components above about 1kHz and below about 10 Hz, where the interferometers’ noise becomes severe).

A British/German group is constructing a 600-meter interferometer called GEO 600 near Hanover Germany [16], and Japanese groups, a 300-meter interferometer called TAMA near Tokyo [17]. GEO600 may be a significant player in the interferometric network in its early years (by virtue of cleverness and speed of construction), but because of its short arms it cannot compete in the long run. GEO600 and TAMA will both be important development centers and testbeds for interferometer techniques and technology, and in due course they may give rise to kilometer-scale interferometers like LIGO and VIRGO, which could significantly enhance the network’s all-sky coverage and ability to extract information from the waves.

3.3 Narrow-Band, High-Frequency Detectors: Interferometers and Resonant-Mass Antennas

At frequencies $f \gtrsim 500\text{Hz}$, the interferometers’ photon shot noise becomes a serious obstacle to wave detection. However, narrow-band detectors specially optimized for kHz frequencies show considerable promise. These include interferometers with specialized optical configurations (“signal recycled interferometers” [18] and “resonant sideband extraction interferometers” [19]), and large spherical or truncated icosahedral resonant-mass detectors (e.g., the American TIGA [20], Dutch GRAIL [21] and Brazilian OMNI-1 Projects) that are future variants of Joseph Weber’s original “bar” detector [1] and of currently operating bars in Italy (AURIGA, Explorer and Nautilus), Australia (NIOBE), and America (ALLEGRO) [22]. Developmental work for these narrow-band detectors is underway at a number of centers around the world.

3.4 Low-Frequency Detectors—The Laser Interferometer Space Antenna (LISA)

The *Laser Interferometer Space Antenna* (LISA) [23] is the most promising detector for gravitational waves in the low-frequency band, 10^{-4} –1 Hz (10,000 times lower than the LIGO/VIRGO high-frequency band).

LISA was originally conceived (under a different name) by Peter Bender of the University of Colorado, and is currently being developed by an international team led by Karsten Danzmann of the University of Hanover (Germany) and James Hough of Glasgow University (UK). The European Space Agency tentatively plans to fly it sometime in the 2014–2018 time frame as part of ESA’s Horizon 2000+ Program of large space missions. With NASA participation (which is

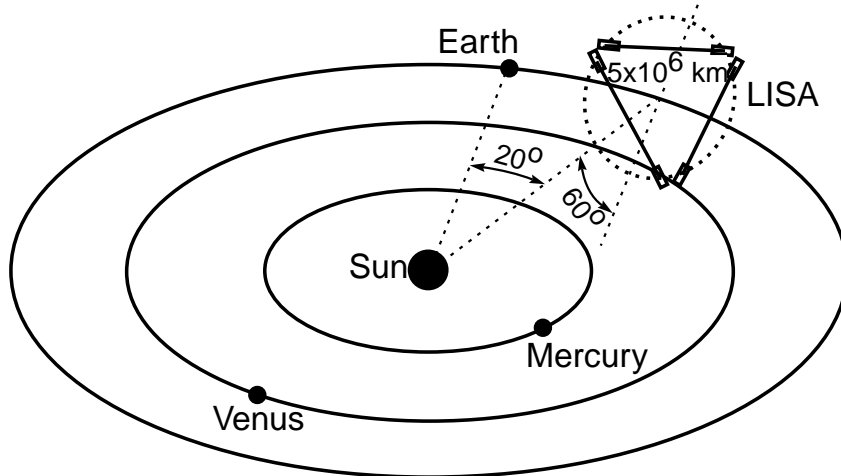


Figure 4: LISA's orbital configuration, with LISA magnified in arm length by a factor ~ 10 relative to the solar system.

under study), the flight could be much sooner.

As presently conceived [23], LISA will consist of six compact, drag-free spacecraft (i.e. spacecraft that are shielded from buffeting by solar wind and radiation pressure, and that thus move very nearly on geodesics of spacetime). All six spacecraft would be launched simultaneously in a single Ariane rocket. They would be placed into the same heliocentric orbit as the Earth occupies, but would follow 20° behind the Earth; cf. Fig. 4. The spacecraft would fly in pairs, with each pair at the vertex of an equilateral triangle that is inclined at an angle of 60° to the Earth's orbital plane. The triangle's arm length would be 5 million km (10^6 times longer than LIGO's arms!). The six spacecraft would track each other optically, using one-Watt YAG laser beams. Because of diffraction losses over the 5×10^6 km arm length, it is not feasible to reflect the beams back and forth between mirrors as is done with LIGO. Instead, each spacecraft would have its own laser; and the lasers would be phase locked to each other, thereby achieving the same kind of phase-coherent out-and-back light travel as LIGO achieves with mirrors. The six-laser, six-spacecraft configuration thereby would function as three, partially independent and partially redundant, gravitational-wave interferometers.

Figure 5 depicts the expected sensitivity of LISA in the same language as we have used for LIGO (Fig. 3): $h_{\text{SB}} = 5\sqrt{5}h_{\text{rms}}$ is the sensitivity for high-confidence detection ($S/N = 5$) of a signal coming from a random direction, assuming Gaussian noise.

At frequencies $f \gtrsim 10^{-3}\text{Hz}$, LISA's noise is due to photon counting statistics (shot noise). The sensitivity curve steepens at $f \sim 3 \times 10^{-2}\text{Hz}$ because at larger f than that, the waves' period is shorter than the round-trip light travel time in one of LISA's arms. Below 10^{-3}Hz , the noise is due to buffeting-induced random motions of the spacecraft that are not being properly removed by the drag-compensation system. Notice that, in terms of dimensionless amplitude, LISA's sensitivity is roughly the same as that of LIGO's first interferometers (Fig. 3), but at 100,000 times lower frequency. Since the waves' energy flux scales as $f^2 h^2$, this corresponds to 10^{10} better energy sensitivity than LIGO.

LISA can detect and study, simultaneously, a wide variety of different sources scattered over all directions on the sky. The key to distinguishing the different sources is the different time evolution of their waveforms. The key to determining each source's direction, and confirming

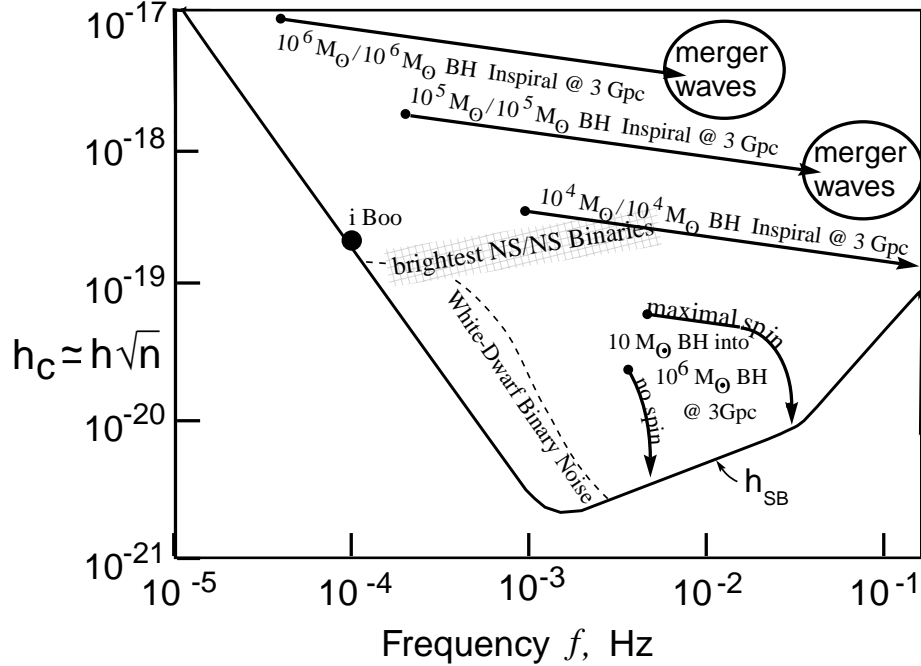


Figure 5: LISA’s projected sensitivity to bursts h_{SB} , compared with the strengths of the waves from several low-frequency sources [23].

that it is real and not just noise, is the manner in which its waves’ amplitude and frequency are modulated by LISA’s complicated orbital motion—a motion in which the interferometer triangle rotates around its center once per year, and the interferometer plane precesses around the normal to the Earth’s orbit once per year. Most sources will be observed for a year or longer, thereby making full use of these modulations.

4 Stellar Core Collapse: The Births of Neutron Stars and Black Holes

In the remainder of this article, I shall describe the techniques and prospects for observationally studying black holes and relativistic stars via the gravitational waves they emit. I begin with the births of stellar-mass neutron stars and black holes.

When the core of a massive star has exhausted its supply of nuclear fuel, it collapses to form a neutron star or a black hole. In some cases, the collapse triggers and powers a subsequent explosion of the star’s mantle—a supernova explosion. Despite extensive theoretical efforts for more than 30 years, and despite wonderful observational data from Supernova 1987A, theorists are still far from a definitive understanding of the details of the collapse and explosion. The details are highly complex and may differ greatly from one core collapse to another [24].

Several features of the collapse and the core’s subsequent evolution can produce significant gravitational radiation in the high-frequency band. We shall consider these features in turn, the most weakly radiating first, and we shall focus primarily on collapses that produce neutron stars rather than black holes.

4.1 Boiling of a Newborn Neutron Star

Even if the collapse is spherical, so it cannot radiate any gravitational waves at all, it should produce a convectively unstable neutron star that “boils” vigorously (and nonspherically) for the first ~ 1 second of its life [25]. The boiling dredges up high-temperature nuclear matter ($T \sim 10^{12}\text{K}$) from the neutron star’s central regions, bringing it to the surface (to the “neutrino-sphere”), where it cools by neutrino emission before being swept back downward and reheated. Burrows [26] has pointed out that the boiling should generate $n \sim 100$ cycles of gravitational waves with frequency $f \sim 100\text{Hz}$ and amplitude large enough to be detectable by LIGO/VIRGO throughout our galaxy and its satellites. Neutrino detectors have a similar range, and there could be a high scientific payoff from correlated observations of the gravitational waves emitted by the boiling’s mass motions and neutrinos emitted from the boiling neutrino-sphere. With neutrinos to trigger on, the sensitivities of LIGO detectors should be about twice as good as shown in Fig. 3.

Recent 3+1 dimensional simulations by Müller and Janka [27] suggest an rms amplitude $h \sim 2 \times 10^{-23}(20\text{kpc}/r)$ (where r is the distance to the source), corresponding to a characteristic amplitude $h_c \simeq h\sqrt{n} \sim 2 \times 10^{-22}(20\text{kpc}/r)$; cf. Fig. 3. (The older 2+1 dimensional simulations gave h_c about 6 times larger than this [27], but presumably were less reliable.) LIGO should be able to detect such waves throughout our galaxy with an amplitude signal to noise ratio of about $S/N = 2.5$ in each of its two enhanced 4km interferometers, and its advanced interferometers should do the same out to 80Mpc distance. (Recall that the h_{SB} curves in Fig. 3 are drawn at a signal to noise ratio of about 5). Although the estimated event rate is only about one every 40 years in our galaxy and not much larger out to 80Mpc, if just one such supernova is detected the correlated neutrino and gravitational wave observations could bring very interesting insights into the boiling of a newborn neutron star.

4.2 Axisymmetric Collapse, Bounce, and Oscillations

Rotation will centrifugally flatten the collapsing core, enabling it to radiate as it implodes. If the core’s angular momentum is small enough that centrifugal forces do not halt or strongly slow the collapse before it reaches nuclear densities, then the core’s collapse, bounce, and subsequent oscillations are likely to be axially symmetric. Numerical simulations [28, 29] show that in this case the waves from collapse, bounce, and oscillation will be quite weak: the total energy radiated as gravitational waves is not likely to exceed $\sim 10^{-7}$ solar masses (about 1 part in a million of the collapse energy) and might often be much less than this; and correspondingly, the waves’ characteristic amplitude will be $h_c \lesssim 3 \times 10^{-21}(30\text{kpc}/r)$. These collapse-and-bounce waves will come off at frequencies $\sim 200\text{ Hz}$ to $\sim 1000\text{ Hz}$, and will precede the boiling waves by a fraction of a second. Though a little stronger than the boiling waves, they probably cannot be seen by LIGO/VIRGO beyond the local group of galaxies and thus will be a very rare occurrence.

4.3 Rotation-Induced Bars and Break-Up

If the core’s rotation is large enough to strongly flatten the core before or as it reaches nuclear density, then a dynamical or secular instability is likely to break the core’s axisymmetry. The core will be transformed into a bar-like configuration that spins end-over-end like an American football, and that might even break up into two or more massive pieces. As we shall see below, the radiation from the spinning bar or orbiting pieces *could* be almost as strong as that from a coalescing neutron-star binary (Sec. 6.2), and thus could be seen by the LIGO/VIRGO first

interferometers out to the distance of the Virgo cluster (where the supernova rate is several per year), by enhanced interferometers out to $\sim 100\text{Mpc}$ (supernova rate several thousand per year), and by advanced interferometers out to several hundred Mpc (supernova rate $\sim (\text{a few}) \times 10^4$ per year); cf. Fig. 3. It is far from clear what fraction of collapsing cores will have enough angular momentum to break their axisymmetry, and what fraction of those will actually radiate at this high rate; but even if only $\sim 1/1000$ or $1/10^4$ do so, this could ultimately be a very interesting source for LIGO/VIRGO.

Several specific scenarios for such non-axisymmetry have been identified:

Centrifugal hangup at $\sim 100\text{km}$ radius: If the pre-collapse core is rapidly spinning (e.g., if it is a white dwarf that has been spun up by accretion from a companion), then the collapse may produce a highly flattened, centrifugally supported disk with most of its mass at radii $R \sim 100\text{km}$, which then (via instability) may transform itself into a bar or may bifurcate. The bar or bifurcated lumps will radiate gravitational waves at twice their rotation frequency, $f \sim 100\text{Hz}$ —the optimal frequency for LIGO/VIRGO interferometers. To shrink on down to $\sim 10\text{km}$ size, this configuration must shed most of its angular momentum. *If* a substantial fraction of the angular momentum goes into gravitational waves, then independently of the strength of the bar, the waves will be nearly as strong as those from a coalescing binary. The reason is this: The waves' amplitude h is proportional to the bar's ellipticity e , the number of cycles n of wave emission is proportional to $1/e^2$, and the characteristic amplitude $h_c = h\sqrt{n}$ is thus independent of the ellipticity and is about the same whether the configuration is a bar or is two lumps [30]. The resulting waves will thus have h_c roughly half as large, at $f \sim 100\text{Hz}$, as the h_c from a NS/NS binary (half as large because each lump might be half as massive as a NS), and the waves will chirp upward in frequency in a manner similar to those from a binary (Sec. 6.2).

It may very well be, however, that most of the core's excess angular momentum does *not* go into gravitational waves, but instead goes largely into hydrodynamic waves as the bar or lumps, acting like a propeller, stir up the surrounding stellar mantle. In this case, the radiation will be correspondingly weaker.

Centrifugal hangup at $\sim 20\text{km}$ radius: Lai and Shapiro [31] have explored the case of centrifugal hangup at radii not much larger than the final neutron star, say $R \sim 20\text{km}$. Using compressible ellipsoidal models, they have deduced that, after a brief period of dynamical bar-mode instability with wave emission at $f \sim 1000\text{Hz}$ (explored by Houser, Centrella, and Smith [32]), the star switches to a secular instability in which the bar's angular velocity gradually slows while the material of which it is made retains its high rotation speed and circulates through the slowing bar. The slowing bar emits waves that sweep *downward* in frequency through the LIGO/VIRGO optimal band $f \sim 100\text{Hz}$, toward $\sim 10\text{Hz}$. The characteristic amplitude (Fig. 3) is only modestly smaller than for the upward-sweeping waves from hangup at $R \sim 100\text{km}$, and thus such waves should be detectable near the Virgo Cluster by the first LIGO/VIRGO interferometers, near 100Mpc by enhanced interferometers, and at distances of a few 100Mpc by advanced interferometers.

Successive fragmentations of an accreting, newborn neutron star: Bonnell and Pringle [33] have focused on the evolution of the rapidly spinning, newborn neutron star as it quickly accretes more and more mass from the pre-supernova star's inner mantle. If the accreting material carries high angular momentum, it may trigger a renewed bar formation, lump formation, wave emission, and coalescence, followed by more accretion, bar and lump formation, wave emission, and coalescence. Bonnell and Pringle speculate that hydrodynamics, not wave emission, will drive this evolution, but that the total energy going into gravitational

waves might be as large as $\sim 10^{-3}M_{\odot}$. This corresponds to $h_c \sim 10^{-21}(10\text{Mpc}/r)$.

5 Pulsars: Spinning Neutron Stars

As the neutron star settles down into its final state, its crust begins to solidify (crystalize). The solid crust will assume nearly the oblate axisymmetric shape that centrifugal forces are trying to maintain, with poloidal ellipticity $\epsilon_p \propto (\text{angular velocity of rotation})^2$. However, the principal axis of the star's moment of inertia tensor may deviate from its spin axis by some small “wobble angle” θ_w , and the star may deviate slightly from axisymmetry about its principal axis; i.e., it may have a slight ellipticity $\epsilon_e \ll \epsilon_p$ in its equatorial plane.

As this slightly imperfect crust spins, it will radiate gravitational waves [34]: ϵ_e radiates at twice the rotation frequency, $f = 2f_{\text{rot}}$ with $h \propto \epsilon_e$, and the wobble angle couples to ϵ_p to produce waves at $f = f_{\text{rot}} + f_{\text{prec}}$ (the precessional sideband of the rotation frequency) with amplitude $h \propto \theta_w \epsilon_p$. For typical neutron-star masses and moments of inertia, the wave amplitudes are

$$h \sim 6 \times 10^{-25} \left(\frac{f_{\text{rot}}}{500\text{Hz}} \right)^2 \left(\frac{1\text{kpc}}{r} \right) \left(\frac{\epsilon_e \text{ or } \theta_w \epsilon_p}{10^{-6}} \right). \quad (3)$$

The neutron star gradually spins down, due in part to gravitational-wave emission but perhaps more strongly due to electromagnetic torques associated with its spinning magnetic field and pulsar emission. This spin-down reduces the strength of centrifugal forces, and thereby causes the star's poloidal ellipticity ϵ_p to decrease, with an accompanying breakage and resolidification of its crust's crystal structure (a “starquake”) [35]. In each starquake, θ_w , ϵ_e , and ϵ_p will all change suddenly, thereby changing the amplitudes and frequencies of the star's two gravitational “spectral lines” $f = 2f_{\text{rot}}$ and $f = f_{\text{rot}} + f_{\text{prec}}$. After each quake, there should be a healing period in which the star's fluid core and solid crust, now rotating at different speeds, gradually regain synchronism. By monitoring the amplitudes, frequencies, and phases of the two gravitational-wave spectral lines, and by comparing with timing of the electromagnetic pulsar emission, one might learn much about the physics of the neutron-star interior.

How large will be the quantities ϵ_e and $\theta_w \epsilon_p$? Rough estimates of the crustal shear moduli and breaking strengths suggest an upper limit in the range $\epsilon_{\text{max}} \sim 10^{-4}$ to 10^{-6} , and it might be that typical values are far below this. We are extremely ignorant, and correspondingly there is much to be learned from searches for gravitational waves from spinning neutron stars.

One can estimate the sensitivity of LIGO/VIRGO (or any other broad-band detector) to the periodic waves from such a source by multiplying the waves' amplitude h by the square root of the number of cycles over which one might integrate to find the signal, $n = f\hat{\tau}$ where $\hat{\tau}$ is the integration time. The resulting effective signal strength, $h\sqrt{n}$, is larger than h by

$$\sqrt{n} = \sqrt{f\hat{\tau}} = 10^5 \left(\frac{f}{1000\text{Hz}} \right)^{1/2} \left(\frac{\hat{\tau}}{4\text{months}} \right)^{1/2}. \quad (4)$$

Four months of integration is not unreasonable in targeted searches; but for an all-sky, all-frequency search, a coherent integration might not last longer than a few days because of computational limitations associated with having to apply huge numbers of trial neutron-star spindown corrections and earth-motion doppler corrections [36].

Equations (3) and (4) for $h\sqrt{n}$ should be compared (i) to the detector's rms broad-band noise level for sources in a random direction, $\sqrt{5}h_{\text{rms}}$, to deduce a signal-to-noise ratio, or (ii) to h_{SB} to deduce a sensitivity for high-confidence detection when one does not know the waves' frequency

in advance [11]. Such a comparison suggests that the first interferometers in LIGO/VIRGO might possibly see waves from nearby spinning neutron stars, but the odds of success are very unclear.

The deepest searches for these nearly periodic waves will be performed by narrow-band detectors, whose sensitivities are enhanced near some chosen frequency at the price of sensitivity loss elsewhere—signal-recycled interferometers [18], resonant-sideband-extraction interferometers [19], or resonant-mass antennas [20, 21] (Section 3.3). With “advanced-detector technology” and targeted searches, such detectors might be able to find with confidence spinning neutron stars that have [11]

$$(\epsilon_e \text{ or } \theta_w \epsilon_p) \gtrsim 3 \times 10^{-10} \left(\frac{500 \text{Hz}}{f_{\text{rot}}} \right)^2 \left(\frac{r}{1000 \text{pc}} \right)^2. \quad (5)$$

There may well be a large number of such neutron stars in our galaxy; but it is also conceivable that there are none. We are extremely ignorant.

Some cause for optimism arises from several physical mechanisms that might generate radiating ellipticities large compared to 3×10^{-10} :

- It may be that, inside the superconducting cores of many neutron stars, there are trapped magnetic fields with mean strength $B_{\text{core}} \sim 10^{13} \text{G}$ or even 10^{15}G . Because such a field is actually concentrated in flux tubes with $B = B_{\text{crit}} \sim 6 \times 10^{14} \text{G}$ surrounded by field-free superconductor, its mean pressure is $p_B = B_{\text{core}} B_{\text{crit}} / 8\pi$. This pressure could produce a radiating ellipticity $\epsilon_e \sim \theta_w \epsilon_p \sim p_B / p \sim 10^{-8} B_{\text{core}} / 10^{13} \text{G}$ (where p is the core’s material pressure).
- Accretion onto a spinning neutron star can drive precession (keeping θ_w substantially nonzero), and thereby might produce measurably strong waves [37].
- If a neutron star is born rotating very rapidly, then it may experience a gravitational-radiation-reaction-driven instability first discovered by Chandrasekhar [38] and elucidated in greater detail by Friedman and Schutz [39]). In this “CFS instability”, density waves travel around the star in the opposite direction to its rotation, but are dragged forward by the rotation. These density waves produce gravitational waves that carry positive energy as seen by observers far from the star, but negative energy from the star’s viewpoint; and because the star thinks it is losing negative energy, its density waves get amplified. This intriguing mechanism is similar to that by which spiral density waves are produced in galaxies. Although the CFS instability was once thought ubiquitous for spinning stars [39, 40], we now know that neutron-star viscosity will kill it, stabilizing the star and turning off the waves, when the star’s temperature is above some limit $\sim 10^{10} \text{K}$ [41] and below some limit $\sim 10^9 \text{K}$ [42]; and correspondingly, the instability should operate only during the first few years of a neutron star’s life, when $10^9 \text{K} \lesssim T \lesssim 10^{10} \text{K}$.

6 Neutron-Star Binaries and Their Coalescence

6.1 NS/NS and Other Compact Binaries in Our Galaxy

The best understood of all gravitational-wave sources are binaries made of two neutron stars (“NS/NS binaries”). The famous Hulse-Taylor [43, 44] binary pulsar, PSR 1913+16, is an example. At present PSR 1913+16 has an orbital frequency of about 1/(8 hours) and emits its

waves predominantly at twice this frequency, roughly 10^{-4} Hz, which is in LISA’s low-frequency band (Fig. 5); but it is too weak for LISA to detect. LISA will be able to search for brighter NS/NS binaries in our galaxy with periods shorter than this.

If conservative estimates [45, 46, 47] based on the statistics of binary pulsar observations are correct, there should be many NS/NS binaries in our galaxy that are brighter in gravitational waves than PSR 1913+16. Those estimates suggest that one compact NS/NS binary is born every 10^5 years in our galaxy and that the brightest NS/NS binaries will fall in the indicated region in Fig. 5, extending out to a high-frequency limit of $\simeq 3 \times 10^{-3}$ Hz (corresponding to a remaining time to coalescence of 10^5 years). The birth rate might be much higher than $1/10^5$ years, according to progenitor evolutionary arguments [46, 48, 49, 50, 51, 52], in which case LISA would see brighter and higher-frequency binaries than shown in Fig. 5. LISA’s observations should easily reveal the true compact NS/NS birth rate and also the birth rates of NS/BH and BH/BH binaries—classes of objects that have not yet been discovered electromagnetically. For further details see [53, 23]; for estimates of LISA’s angular resolution when observing such binaries, see [54].

6.2 The Final Inspiral of a NS/NS Binary

As a result of their loss of orbital energy to gravitational waves, the PSR 1913+16 NS’s are gradually spiraling inward at a rate that agrees with general relativity’s prediction to within the measurement accuracy (a fraction of a percent) [44]—a remarkable but indirect confirmation that gravitational waves do exist and are correctly described by general relativity. If we wait roughly 10^8 years, this inspiral will bring the waves into the LIGO/ VIRGO high-frequency band. As the NS’s continue their inspiral, over a time of about 15 minutes the waves will sweep through the LIGO/VIRGO band, from ~ 10 Hz to $\sim 10^3$ Hz, at which point the NS’s will collide and merge. It is this last 15 minutes of inspiral, with $\sim 16,000$ cycles of waveform oscillation, and the final merger, that the LIGO/VIRGO network seeks to monitor.

To what distance must LIGO/VIRGO look, in order to see such inspirals several times per year? Beginning with our galaxy’s conservative, pulsar-observation-based NS/NS event rate of one every 100,000 years (Sec. 6.1) and extrapolating out through the Universe, one infers an event rate of several per year at 200 Mpc [45, 46, 47]. If arguments based on simulations of binary evolution are correct [46, 48, 49, 50, 51, 52] (Sec. 6.1), the distance for several per year could be as small as 23 Mpc—though such a small distance entails stretching all the numbers to near their breaking point of plausibility [46]. If one stretches all numbers to the opposite, most pessimistic extreme, one infers several per year at 1000 Mpc [46]. Whatever may be the true distance for several per year, once LIGO/VIRGO reaches that distance, each further improvement of sensitivity by a factor 2 will increase the observed event rate by $2^3 \simeq 10$.

Figure 3 compares the projected LIGO sensitivities [12] with the wave strengths from NS/NS inspirals at various distances from Earth. From that comparison we see that LIGO’s first interferometers can reach 30Mpc, where the most extremely optimistic estimates predict several per year; the enhanced interferometers can reach 300Mpc where the binary-pulsar-based, conservative estimates predict ~ 10 per year; the advanced interferometers can reach 1000Mpc where even the most extremely pessimistic of estimates predict several per year.

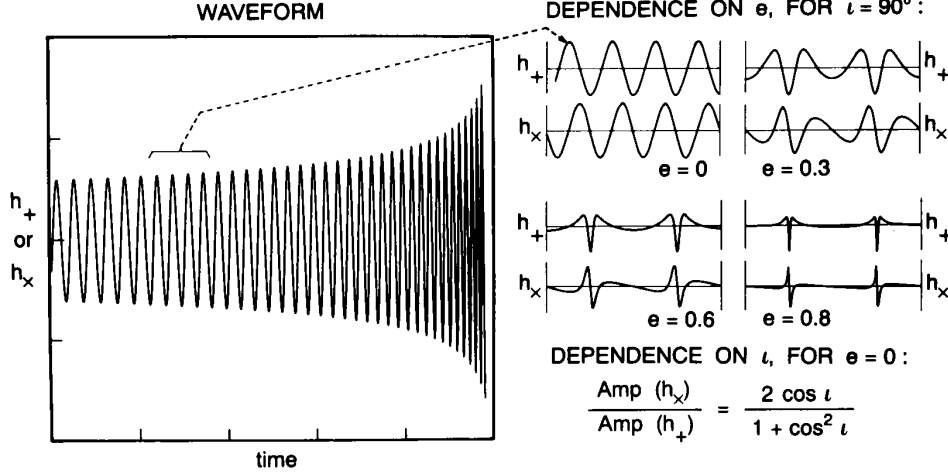


Figure 6: Waveforms from the inspiral of a compact binary (NS/NS, NS/BH, or BH/BH), computed using Newtonian gravity for the orbital evolution and the quadrupole-moment approximation for the wave generation. (From Ref. [12].)

6.3 Inspiral Waveforms and the Information they Carry

Neutron stars have such intense self gravity that it is exceedingly difficult to deform them. Correspondingly, as they spiral inward in a compact binary, they do not gravitationally deform each other significantly until several orbits before their final coalescence [55, 56]. This means that the inspiral waveforms are determined to high accuracy by only a few, clean parameters: the masses and spin angular momenta of the stars, and the initial orbital elements (i.e. the elements when the waves enter the LIGO/VIRGO band). The same is true for NS/BH and BH/BH binaries. The following description of inspiral waveforms is independent of whether the binary’s bodies are NS’s or BH’s.

Though tidal deformations are negligible during inspiral, relativistic effects can be very important. If, for the moment, we ignore the relativistic effects—i.e., if we approximate gravity as Newtonian and the wave generation as due to the binary’s oscillating quadrupole moment [11], then the shapes of the inspiral waveforms $h_+(t)$ and $h_\times(t)$ are as shown in Fig. 6.

The left-hand graph in Fig. 6 shows the waveform increasing in amplitude and sweeping upward in frequency (i.e., undergoing a “chirp”) as the binary’s bodies spiral closer and closer together. The ratio of the amplitudes of the two polarizations is determined by the inclination i of the orbit to our line of sight (lower right in Fig. 6). The shapes of the individual waves, i.e. the waves’ harmonic content, are determined by the orbital eccentricity (upper right). (Binaries produced by normal stellar evolution should be highly circular due to past radiation reaction forces, but compact binaries that form by capture events, in dense star clusters that might reside in galactic nuclei [57], could be quite eccentric.) If, for simplicity, the orbit is circular, then the rate at which the frequency sweeps or “chirps”, df/dt [or equivalently the number of cycles spent near a given frequency, $n = f^2(df/dt)^{-1}$] is determined solely, in the Newtonian/quadrupole approximation, by the binary’s so-called *chirp mass*, $M_c \equiv (M_1 M_2)^{3/5} / (M_1 + M_2)^{1/5}$ (where M_1 and M_2 are the two bodies’ masses). The amplitudes of the two waveforms are determined by the chirp mass, the distance to the source, and the orbital inclination. Thus (in the Newtonian/quadrupole approximation), by measuring the two amplitudes, the frequency sweep, and the harmonic content of the inspiral waves, one can determine as direct, resulting observables,

the source’s distance, chirp mass, inclination, and eccentricity [58, 30]. (For binaries at cosmological distances, the observables are the “luminosity distance,” “redshifted” chirp mass $(1+z)M_c$, inclination, and eccentricity; cf. Sec. 7.2.)

As in binary pulsar observations [44], so also here, relativistic effects add further information: they influence the rate of frequency sweep and produce waveform modulations in ways that depend on the binary’s dimensionless ratio $\eta = \mu/M$ of reduced mass $\mu = M_1 M_2 / (M_1 + M_2)$ to total mass $M = M_1 + M_2$ and on the spins of the binary’s two bodies. These relativistic effects are reviewed and discussed at length in Refs. [59, 60]. Two deserve special mention: (i) As the waves emerge from the binary, some of them get backscattered one or more times off the binary’s spacetime curvature, producing wave *tails*. These tails act back on the binary, modifying its radiation reaction force and thence its inspiral rate in a measurable way. (ii) If the orbital plane is inclined to one or both of the binary’s spins, then the spins drag inertial frames in the binary’s vicinity (the “Lense-Thirring effect”), this frame dragging causes the orbit to precess, and the precession modulates the waveforms [59, 61, 62].

Remarkably, the relativistic corrections to the frequency sweep—tails, spin-induced precession and others—will be measurable with rather high accuracy, even though they are typically $\lesssim 10$ per cent of the Newtonian contribution, and even though the typical signal to noise ratio will be only ~ 9 . The reason is as follows [63, 64, 59]:

The frequency sweep will be monitored by the method of “matched filters”; in other words, the incoming, noisy signal will be cross correlated with theoretical templates. If the signal and the templates gradually get out of phase with each other by more than $\sim 1/10$ cycle as the waves sweep through the LIGO/VIRGO band, their cross correlation will be significantly reduced. Since the total number of cycles spent in the LIGO/VIRGO band will be $\sim 16,000$ for a NS/NS binary, ~ 3500 for NS/BH, and ~ 600 for BH/BH, this means that LIGO/VIRGO should be able to measure the frequency sweep to a fractional precision $\lesssim 10^{-4}$, compared to which the relativistic effects are very large. (This is essentially the same method as Joseph Taylor and colleagues use for high-accuracy radio-wave measurements of relativistic effects in binary pulsars [44].)

Analyses using the theory of optimal signal processing predict the following typical accuracies for LIGO/VIRGO measurements based solely on the frequency sweep (i.e., ignoring modulational information) [65]: (i) The chirp mass M_c will typically be measured, from the Newtonian part of the frequency sweep, to $\sim 0.04\%$ for a NS/NS binary and $\sim 0.3\%$ for a system containing at least one BH. (ii) *If* we are confident (e.g., on a statistical basis from measurements of many previous binaries) that the spins are a few percent or less of the maximum physically allowed, then the reduced mass μ will be measured to $\sim 1\%$ for NS/NS and NS/BH binaries, and $\sim 3\%$ for BH/BH binaries. (Here and below NS means a $\sim 1.4M_\odot$ neutron star and BH means a $\sim 10M_\odot$ black hole.) (iii) Because the frequency dependences of the (relativistic) μ effects and spin effects are not sufficiently different to give a clean separation between μ and the spins, if we have no prior knowledge of the spins, then the spin/ μ correlation will worsen the typical accuracy of μ by a large factor, to $\sim 30\%$ for NS/NS, $\sim 50\%$ for NS/BH, and a factor ~ 2 for BH/BH. These worsened accuracies might be improved somewhat by waveform modulations caused by the spin-induced precession of the orbit [61, 62], and even without modulational information, a certain combination of μ and the spins will be determined to a few per cent. Much additional theoretical work is needed to firm up the measurement accuracies.

To take full advantage of all the information in the inspiral waveforms will require theoretical templates that are accurate, for given masses and spins, to a fraction of a cycle during the entire sweep through the LIGO/VIRGO band. Such templates are being computed by an international

consortium of relativity theorists (Blanchet and Damour in France, Iyer in India, Will and Wiseman in the U.S.) [66], using post-Newtonian expansions of the Einstein field equations, of the sort pioneered by Chandrasekhar [67, 68]. This enterprise is rather like computing the Lamb shift to high order in powers of the fine structure constant, for comparison with experiment and testing of quantum electrodynamics. Cutler and Flanagan [69] have estimated the order to which the computations must be carried in order that systematic errors in the theoretical templates will not significantly impact the information extracted from the LIGO/VIRGO observational data. The answer appears daunting: radiation-reaction effects must be computed to three full post-Newtonian orders [six orders in $v/c = (\text{orbital velocity})/(\text{speed of light})$] beyond Chandra's leading-order radiation reaction, which itself is 5 orders in v/c beyond the Newtonian theory of gravity, so the required calculations are $O[(v/c)^{6+5}] = O[(v/c)^{11}]$. By clever use of Padé approximates, these requirements might be relaxed [70].

In the late 1960's, when Chandra and I were first embarking on our respective studies of gravitational waves, Chandra set out to compute the first 5 orders in v/c beyond Newton, i.e., in his own words, "to solve Einstein's equations through the 5/2 post-Newtonian", thereby fully understanding leading-order radiation reaction and all effects leading up to it. Some colleagues thought his project not worth the enormous personal effort that he put into it. But Chandra was prescient. He had faith in the importance of his effort, and history has proved him right. The results of his "5/2 post-Newtonian" [68] calculation have now been verified to accuracy better than 1% by observations of the inspiral of PSR 1913+16; and the needs of LIGO/VIRGO data analysis are now driving the calculations onward from $O[(v/c)^5]$ to $O[(v/c)^{11}]$. This epitomizes a major change in the field of relativity research: At last, 80 years after Einstein formulated general relativity, experiment has become a major driver for theoretical analyses.

Remarkably, the goal of $O[(v/c)^{11}]$ is achievable. The most difficult part of the computation, the radiation reaction, has been evaluated to $O[(v/c)^9]$ beyond Newton by the French/Indian/American consortium [66] and $O[(v/c)^{11}]$ is now being pursued.

These high-accuracy waveforms are needed only for extracting information from the inspiral waves after the waves have been discovered; they are not needed for the discovery itself. The discovery is best achieved using a different family of theoretical waveform templates, one that covers the space of potential waveforms in a manner that minimizes computation time instead of a manner that ties quantitatively into general relativity theory [59, 71]. Such templates are under development.

6.4 NS/NS Merger Waveforms and their Information

The final merger of a NS/NS binary should produce waves that are sensitive to the equation of state of nuclear matter, so such mergers have the potential to teach us about the nuclear equation of state [12, 59]. In essence, LIGO/VIRGO will be studying nuclear physics via the collisions of atomic nuclei that have nucleon numbers $A \sim 10^{57}$ —somewhat larger than physicists are normally accustomed to. The accelerator used to drive these "nuclei" up to half the speed of light is the binary's self gravity, and the radiation by which the details of the collisions are probed is gravitational.

Unfortunately, the NS/NS merger will emit its gravitational waves in the kHz frequency band ($600\text{Hz} \lesssim f \lesssim 2500\text{Hz}$) where photon shot noise will prevent the waves from being studied by the standard, "workhorse," broad-band interferometers of Fig. 3. However, it may be possible to measure the waves and extract their equation-of-state information using a "xylophone" of specially configured narrow-band detectors (signal-recycled or resonant-sideband-extraction

interferometers, and/or spherical or icosahedral resonant-mass detectors; Sec. 3.3 and Refs. [59, 72]). Such measurements will be very difficult and are likely only when the LIGO/VIRGO network has reached a mature stage.

A number of research groups [73] are engaged in numerical simulations of NS/NS mergers, with the goal not only to predict the emitted gravitational waveforms and their dependence on equation of state, but also (more immediately) to learn whether such mergers might power the γ -ray bursts that have been a major astronomical puzzle since their discovery in the early 1970s.

NS/NS mergers are a promising explanation for γ -ray bursts because (i) some bursts are known, from intergalactic absorption lines, to come from cosmological distances [74], (ii) the bursts have a distribution of number versus intensity that suggests most lie at near-cosmological distances, (iii) their event rate is roughly the same as that conservatively estimated for NS/NS mergers (~ 1000 per year out to cosmological distances; a few per year at 300Mpc); and (iv) it is plausible that the final NS/NS merger will create a γ -emitting fireball with enough energy to account for the bursts [75, 76]. If enhanced LIGO interferometers were now in operation and observing NS/NS inspirals, they could report definitively whether or not the γ -bursts are produced by NS/NS binaries; and if the answer were yes, then the combination of γ -burst data and gravitational-wave data could bring valuable information that neither could bring by itself. For example, it would reveal when, to within a few msec, the γ -burst is emitted relative to the moment the NS's first begin to touch; and by comparing the γ and gravitational times of arrival, we could test whether gravitational waves propagate with the speed of light to a fractional precision of $\sim 0.01\text{sec}/10^9\text{lyr} = 3 \times 10^{-19}$.

6.5 NS/BH Mergers

A neutron star (NS) spiraling into a black hole of mass $M \gtrsim 10M_\odot$ should be swallowed more or less whole. However, if the BH is less massive than roughly $10M_\odot$, and especially if it is rapidly rotating, then the NS will tidally disrupt before being swallowed. Little is known about the disruption and accompanying waveforms. To model them with any reliability will likely require full numerical relativity, since the circumferences of the BH and NS will be comparable and their physical separation at the moment of disruption will be of order their separation. As with NS/NS, the merger waves should carry equation of state information and will come out in the kHz band, where their detection will require advanced, specialty detectors.

7 Black Hole Binaries

7.1 BH/BH Inspiral, Merger, and Ringdown

We turn, next, to binaries made of two black holes with comparable masses (BH/BH binaries). The LIGO/VIRGO network can detect and study waves from the last few minutes of the life of such a binary if its total mass is $M \lesssim 1000M_\odot$ (“stellar-mass black holes”), cf. Fig. 3; and LISA can do the same for the mass range $1000M_\odot \lesssim M \lesssim 10^8M_\odot$ (“supermassive black holes”), cf. Fig. 5.

The timescales for the binary’s dynamics and its waveforms are proportional to its total mass M . All other aspects of the dynamics and waveforms, after time scaling, depend solely on quantities that are dimensionless in geometrized units ($G = c = 1$): the ratio of the two BH masses, the BH spins divided by the squares of their masses, etc. Consequently, the black-hole physics to be studied is the same for supermassive holes in LISA’s low-frequency band as for

stellar-mass holes in LIGO/VIRGO’s high-frequency band. LIGO/VIRGO is likely to make moderate-accuracy studies of this physics; and LISA, flying later, can achieve high accuracy.

The binary’s dynamics and its emitted waveforms can be divided into three epochs: *inspiral*, *merger*, and *ringdown* [77]. The inspiral epoch terminates when the holes reach their last stable orbit and begin plunging toward each other. The merger epoch lasts from the beginning of plunge until the holes have merged and can be regarded as a single hole undergoing large-amplitude, quasinormal-mode vibrations. In the ringdown epoch, the hole’s vibrations decay due to wave emission, leaving finally a quiescent, spinning black hole.

The inspiral epoch has been well studied theoretically using post-Newtonian expansions (Sec. 6.3), except for the last factor ~ 3 of upward frequency sweep, during which the post-Newtonian expansions may fail. The challenge of computing this last piece of the inspiral is called the “intermediate binary black hole problem” (IBBH) and is a subject of current research in my own group and elsewhere. The merger epoch can be studied theoretically only via supercomputer simulations. Techniques for such simulations are being developed by several research groups, including an eight-university American consortium of numerical relativists and computer scientists called the Binary Black Hole Grand Challenge Alliance [78]. Chandrasekhar and Detweiler [79, 80] pioneered the study of the ringdown epoch using the Teukolsky formalism for first-order perturbations of spinning (Kerr) black holes (see Chandra’s classic book [81]), and the ringdown is now rather well understood except for the strengths of excitation of the various vibrational modes, which the merger observations and computations should reveal.

The merger epoch, as yet, is very poorly understood. We can expect it to consist of large-amplitude, highly nonlinear vibrations of spacetime curvature—a phenomenon of which we have very little theoretical understanding today. Especially fascinating will be the case of two spinning black holes whose spins are not aligned with each other or with the orbital angular momentum. Each of the three angular momentum vectors (two spins, one orbital) will drag space in its vicinity into a tornado-like swirling motion—the general relativistic “dragging of inertial frames”—so the binary is rather like two tornados with orientations skewed to each other, embedded inside a third, larger tornado with a third orientation. The dynamical evolution of such a complex configuration of coalescing spacetime warpage, as revealed by its emitted waves, might bring us surprising new insights into relativistic gravity [12].

7.2 BH/BH Signal Strengths and Detectability

Flanagan and Hughes [77] have recently estimated the signal strengths produced in LIGO and in LISA by the waves from equal-mass BH/BH binaries for each of the three epochs, inspiral, merger, and ringdown; and along with signal strengths, they have estimated the distances to which LIGO and LISA can detect the waves. In their estimates, Flanagan and Hughes make plausible assumptions about the waves’ unknown aspects. The estimated signal strengths are shown in Fig. 7 for the first LIGO interferometers, Fig. 8 for advanced LIGO interferometers, and Fig. 9 for LISA. Because LIGO and LISA can both reach out to cosmological distances, these figures are drawn in a manner that includes cosmological effects: they are valid for any homogeneous, isotropic model of our universe. This is achieved by plotting observables that are extracted from the measured waveforms: the binary’s “redshifted” total mass $(1+z)M$ on the horizontal axis (where z is the source’s cosmological redshift) and its “luminosity distance” [82] on the right axis. The signal-to-noise ratio (left axis) scales inversely with the luminosity distance.

We have no good observational handle on the coalescence rate of stellar-mass BH/BH bina-

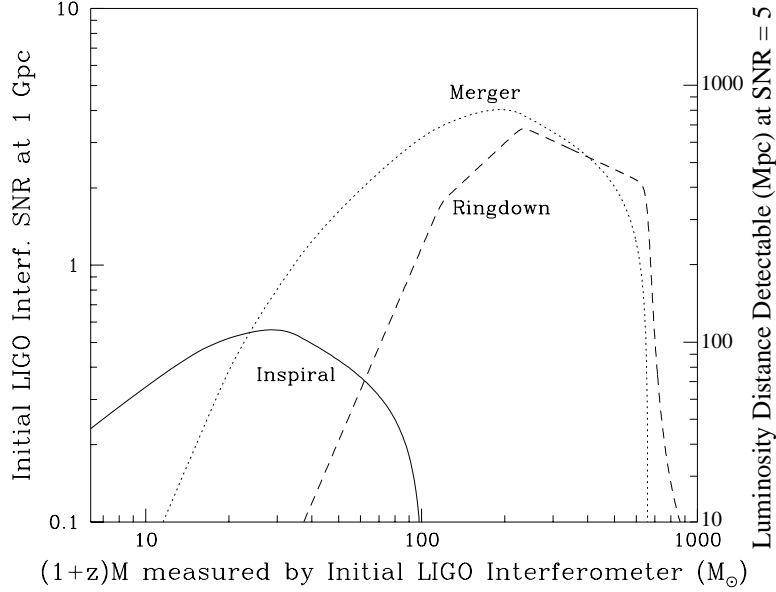


Figure 7: The inspiral, merger, and ringdown waves from equal-mass black-hole binaries as observed by LIGO’s initial interferometers: The luminosity distance to which the waves are detectable (right axis) and the signal-to-noise ratio for a binary at 1Gpc (left axis), as functions of the binary’s redshifted total mass (bottom axis). (Figure adapted from Flanagan and Hughes [77].)

ries. However, for BH/BH binaries with total mass $M \sim 5$ to $50M_{\odot}$ that arise from ordinary main-sequence progenitors, estimates based on the progenitors’ birth rates and on simulations of their subsequent evolution suggest a coalescence rate in our galaxy of one per (1 to 30) million years [51, 48]. These rough estimates imply that to see one coalescence per year with $M \sim 5$ to $50M_{\odot}$, LIGO/VIRGO must reach out to a distance $\sim (300$ to $900)$ Mpc. Other plausible scenarios (e.g. BH/BH binary formation in dense stellar clusters that reside in globular clusters and galactic nuclei [57]) could produce higher event rates and larger masses, but little reliable is known about them (cf. Sec. I.A.ii of [77]).

For comparison, the first LIGO interferometers can reach 300Mpc for $M = 50M_{\odot}$ but only 40Mpc for $M = 5M_{\odot}$ (Fig. 7); enhanced interferometers can reach about 10 times farther, and advanced interferometers about 30 times farther (Fig. 8). These numbers suggest that (i) if waves from BH/BH coalescences are not detected by the first LIGO/VIRGO interferometers, they are likely to be detected along the way from the first interferometers to the enhanced; and (ii) BH/BH coalescences might be detected sooner than NS/NS coalescences (cf. Sec. 6.2).

For binaries with $M(1+z) \gtrsim 40M_{\odot}$, the highly interesting merger signal should be stronger than the inspiral signal, and for $M \gtrsim 100M_{\odot}$, the ringdown should be stronger than inspiral (Fig. 7). Thus, it may well be that early in the life of the LIGO/VIRGO network, observers and theorists will be struggling to understand the merger of binary black holes by comparison of computed and observed waveforms.

LIGO’s advanced interferometers (Fig. 8) can see the merger waves, for $20M_{\odot} \lesssim M \lesssim 200M_{\odot}$ out to a cosmological redshift $z \simeq 5$; and for binaries at $z = 1$ in this mass range, they can achieve a signal to noise ratio (assuming optimal signal processing [77]) of about 25 in each interferometer.

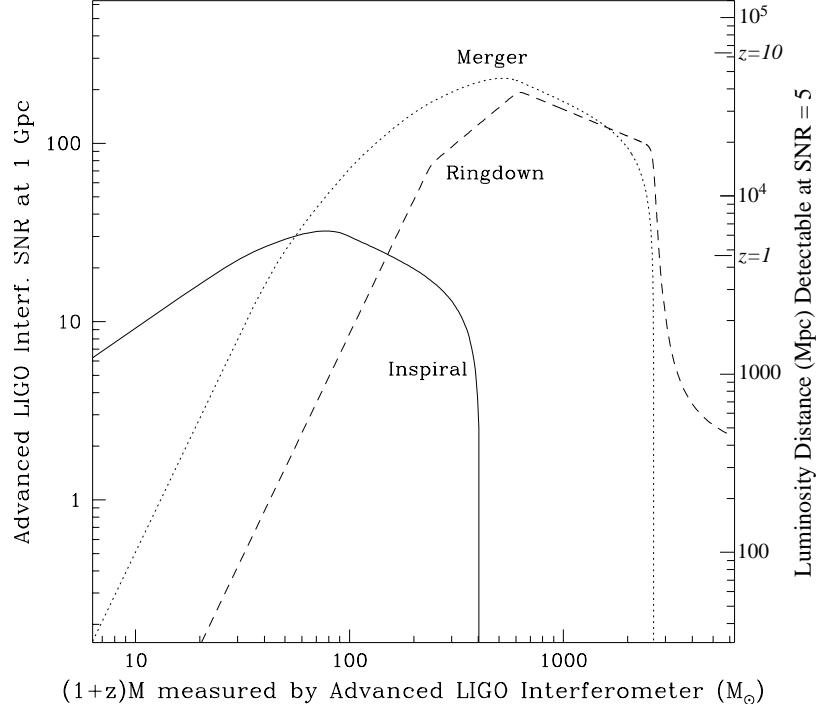


Figure 8: The waves from equal-mass black-hole binaries as observed by LIGO’s advanced interferometers; cf. the caption for Fig. 7. On the right side is shown not only the luminosity distance to which the signals can be seen (valid for any homogeneous, isotropic cosmology), but also the corresponding cosmological redshift z , assuming vanishing cosmological constant, a spatially flat universe, and a Hubble constant $H_o = 75$ km/s/Mpc. (Figure adapted from Flanagan and Hughes [77].)

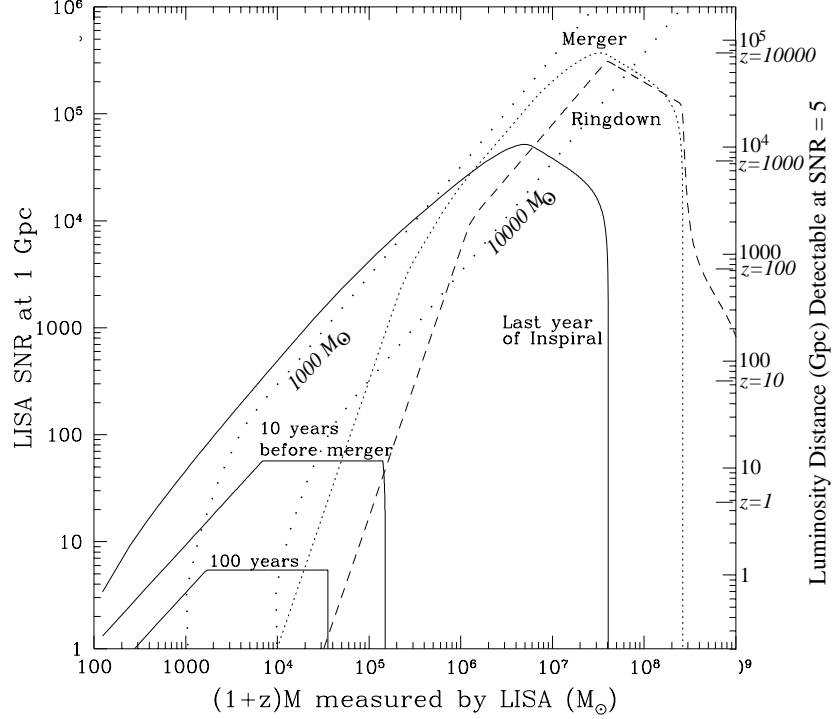


Figure 9: The waves from equal-mass, supermassive black-hole binaries as observed by LISA in one year of integration time; cf. the captions for Figs. 7 and 8. The wide-spaced dots are curves of constant binary mass M , for use with the right axis, assuming vanishing cosmological constant, a spatially flat universe, and a Hubble constant $H_o = 75$ km/s/Mpc. The bottom-most curves are the signal strengths after one year of signal integration, for BH/BH binaries 10 years and 100 years before their merger. (Figure adapted from Flanagan and Hughes [77].)

While these numbers are impressive, they pale by comparison with LISA (Fig. 9), which can detect the merger waves for $1000M_\odot \lesssim M \lesssim 10^5M_\odot$ out to redshifts $z \sim 3000$ (far earlier in the life of the universe than the era when the first supermassive black holes are likely to have formed). Correspondingly, LISA can achieve signal to noise ratios of thousands for mergers with $10^5 \lesssim M \lesssim 10^8M_\odot$ at redshifts of order unity, and from the inspiral waves can infer the binary's parameters (redshifted masses, luminosity distance, direction, ...) with high accuracy [54].

Unfortunately, it is far from obvious whether the event rate for such supermassive BH/BH coalescences will be interestingly high. Conservative estimates suggest a rate of $\sim 0.1/\text{yr}$, while plausible scenarios for aspects of the universe about which we are rather ignorant can give rates as high as $1000/\text{yr}$ [83].

If the coalescence rate is only $0.1/\text{yr}$, then LISA should still see ~ 3 BH/BH binaries with $3000M_\odot \lesssim M \lesssim 10^5M_\odot$ that are ~ 30 years away from their final merger. These slowly inspiraling binaries should be visible, with one year of integration, out to a redshift $z \sim 1$ (bottom part of Fig. 9).

8 Payoffs from Binary Coalescence Observations

Among the scientific payoffs that should come from LIGO/VIRGO’s and/or LISA’s observations of binary coalescence are the following; others have been discussed above.

8.1 Christodoulou Memory

As the gravitational waves from a binary’s coalescence depart from their source, the waves’ energy creates (via the nonlinearity of Einstein’s field equations) a secondary wave called the “Christodoulou memory” [84, 85, 86]. This memory, arriving at Earth, can be regarded rigorously as the combined gravitational field of all the gravitons that have been emitted in directions other than toward the Earth [85]. The memory builds up on the timescale of the primary energy emission profile, and grows most rapidly when the primary waves are being emitted most strongly: during the end of inspiral and the merger. Unfortunately, the memory is so weak that in LIGO only advanced interferometers have much chance of detecting and studying it—and then, only for BH/BH coalescences and not for NS/NS [87]. LISA, by contrast, should easily be able to measure the memory from supermassive BH/BH coalescences.

8.2 Testing General Relativity

Corresponding to the very high post-Newtonian order to which a binary’s inspiral waveforms must be computed for use in LIGO/VIRGO and LISA data analysis (Sec. 6.3), measurements of the inspiral waveforms can be used to test general relativity with very high accuracy. For example, in scalar-tensor theories (some of which are attractive alternatives to general relativity [88]), radiation reaction due to emission of scalar waves places a unique signature on the measured inspiral waveforms—a signature that can be searched for with high precision [89]. Similarly, the inspiral waveforms can be used to measure with high accuracy several fascinating general relativistic phenomena in addition to the Christodoulou memory: the influence of the tails of the emitted waves on radiation reaction in the binary (Sec. 6.3), the Lens-Thirring orbital precession induced by the binary’s spins (Sec. 6.3), and a unique relationship among the multipole moments of a quiescent black hole which is dictated by a hole’s “two-hair theorem” (Sec. 8.4).

The ultimate test of general relativity will be detailed comparisons of the predicted and observed waveforms from the highly nonlinear spacetime-warpage vibrations of BH/BH mergers (Sec. 7.1).

8.3 Cosmological Measurements

Binary inspiral waves can be used to measure the Universe’s Hubble constant, deceleration parameter, and cosmological constant [58, 30, 90, 91]. The keys to such measurements are that: (i) Advanced interferometers in LIGO/VIRGO will be able to see NS/NS inspirals out to cosmological redshifts $z \sim 0.3$, and NS/BH out to $z \sim 2$. (ii) The direct observables that can be extracted from the observed waveforms include a source’s luminosity distance (measured to an accuracy ~ 10 per cent in a large fraction of cases), and its direction on the sky (to accuracy ~ 1 square degree)—accuracies good enough that only one or a few electromagnetically-observed clusters of galaxies should fall within the 3-dimensional gravitational error boxes. This should make possible joint gravitational/electromagnetic statistical studies of our Universe’s magnitude-redshift relation, with gravity giving luminosity distances and electromagnetism giving the redshifts [58, 30]. (iii) Another direct gravitational observable is any redshifted mass $(1+z)M$ in the system. Since

the masses of NS’s in binaries seem to cluster around $1.4M_\odot$, measurements of $(1+z)M$ can provide a handle on the redshift, even in the absence of electromagnetic aid; so gravitational-wave observations alone may be used, in a statistical way, to measure the magnitude-redshift relation [90, 91].

LISA, with its ability to detect BH/BH binaries with $M \sim 1000$ to $100,000M_\odot$ out to redshifts of thousands, could search for the earliest epochs of supermassive black hole activity—if the Universe is kind enough to grant us a large event rate.

8.4 Mapping Quiescent Black Holes; Searching for Exotic Relativistic Bodies

Ryan [92] has shown that, when a white dwarf, neutron star or small black hole spirals into a much more massive, compact central body, the inspiral waves will carry a “map” of the massive body’s external spacetime geometry. Since the body’s spacetime geometry is uniquely characterized by the values of the body’s multiple moments, we can say equivalently that the inspiral waves carry, encoded in themselves, the values of all the body’s multipole moments.

By measuring the inspiral waveforms and extracting their map (i.e., measuring the lowest few multipole moments), we can determine whether the massive central body is a black hole or some other kind of exotic compact object [92]; see below.

The inspiraling object’s orbital energy E at fixed frequency f (and correspondingly at fixed orbital radius a) scales as $E \propto \mu$, where μ is the object’s mass; the gravitational-wave luminosity \dot{E} scales as $\dot{E} \propto \mu^2$; and the time to final merger thus scales as $t \sim E/\dot{E} \propto 1/\mu$. This means that the smaller is μ/M (where M is the central body’s mass), the more orbits are spent in the central body’s strong-gravity region, $a \lesssim 10GM/c^2$, and thus the more detailed and accurate will be the map of the body’s spacetime geometry encoded in the emitted waves.

For holes observed by LIGO/VIRGO, the most extreme mass ratio that we can hope for is $\mu/M \sim 1M_\odot/300M_\odot$, since for $M > 300M_\odot$ the inspiral waves are pushed to frequencies below the LIGO/VIRGO band. This limit on μ/M seriously constrains the accuracy with which LIGO/VIRGO can hope to map the spacetime geometry. A detailed study by Ryan [93] (but one that is rather approximate because we do not know the full details of the waveforms) suggests that LIGO/VIRGO might *not* be able to distinguish cleanly between quiescent black holes and other types of massive central bodies.

By contrast, LISA can observe the final inspiral waves from objects of any mass $\mu \gtrsim 1M_\odot$ spiraling into central bodies of mass $3 \times 10^5 M_\odot \lesssim M \lesssim 3 \times 10^7 M_\odot$ out to 3Gpc. Figure 5 shows the example of a $10M_\odot$ black hole spiraling into a $10^6 M_\odot$ black hole at 3Gpc distance. The inspiral orbit and waves are strongly influenced by the hole’s spin. Two cases are shown [94]: an inspiraling circular orbit around a non-spinning hole, and a prograde, circular, equatorial orbit around a maximally spinning hole. In each case the dot at the upper left end of the arrowed curve is the frequency and characteristic amplitude one year before the final coalescence. In the nonspinning case, the small hole spends its last year spiraling inward from $r \simeq 7.4GM/c^2$ (3.7 Schwarzschild radii) to its last stable circular orbit at $r = 6GM/c^2$ (3 Schwarzschild radii). In the maximal spin case, the last year is spent traveling from $r = 6GM/c^2$ (3 Schwarzschild radii) to the last stable orbit at $r = GM/c^2$ (half a Schwarzschild radius). The $\sim 10^5$ cycles of waves during this last year should carry, encoded in themselves, rather accurate values for the massive hole’s lowest few multipole moments [92, 93] (or, equivalently, a rather accurate map of the hole’s spacetime geometry).

If the measured moments satisfy the black-hole “two-hair” theorem (usually incorrectly called the “no-hair” theorem), i.e. if they are all determined uniquely by the measured mass and spin

in the manner of the Kerr metric, then we can be sure the central body is a black hole. If they violate the two-hair theorem, then (assuming general relativity is correct), either the central body was an exotic object—e.g. a spinning boson star which should have three “hairs” [95], a soliton star [96] or a naked singularity—rather than a black hole, or else an accretion disk or other material was perturbing its orbit [97]. From the evolution of the waves one can hope to determine which is the case, and to explore the properties of the central body and its environment [98].

Models of galactic nuclei, where massive holes (or other massive central bodies) reside, suggest that inspiraling stars and small holes typically will be in rather eccentric orbits [99, 100]. This is because they get injected into such orbits via gravitational deflections off other stars, and by the time gravitational radiation reaction becomes the dominant orbital driving force, there is not enough inspiral left to strongly circularize their orbits. Such orbital eccentricity will complicate the waveforms and complicate the extraction of information from them. Efforts to understand the emitted waveforms, for central bodies with arbitrary multipole moments, are just now getting underway [92, 101]. Even for central black holes, those efforts are at an early stage; for example, only recently have we learned how to compute the influence of radiation reaction on inspiraling objects in fully relativistic, nonequatorial orbits around a black hole [102, 103].

The event rates for inspiral into supermassive black holes (or other supermassive central bodies) are not well understood. However, since a significant fraction of all galactic nuclei are thought to contain supermassive holes, and since white dwarfs and neutron stars, as well as small black holes, can withstand tidal disruption as they plunge toward a supermassive hole’s horizon, and since LISA can see inspiraling bodies as small as $\sim 1M_\odot$ out to 3Gpc distance, the event rate is likely to be interestingly large. Sigurdsson and Rees give a “very conservative” estimate of one inspiral event per year within 1Gpc distance, and 100–1000 sources detectable by LISA at lower frequencies “en route” toward their final plunge.

9 Conclusion

It is now 37 years since Joseph Weber initiated his pioneering development of gravitational-wave detectors [1], 26 years since Robert Forward [104] and Rainer Weiss [2] initiated work on interferometric detectors, and about 35 years since Chandra and others launched the modern era of theoretical research on relativistic stars and black holes. Since then, hundreds of talented experimental physicists have struggled to improve the sensitivities of gravitational-wave detectors, and hundreds of theorists have explored general relativity’s predictions for stars and black holes.

These two parallel efforts are now intimately intertwined and are pushing toward an era in the not distant future, when measured gravitational waveforms will be compared with theoretical predictions to learn how many and what kinds of relativistic objects *really* populate our Universe, and how these relativistic objects *really* are structured and *really* behave when quiescent, when vibrating, and when colliding.

10 Acknowledgments

My group’s research on gravitational waves and their relevance to LIGO/VIRGO and LISA is supported in part by NSF grants AST-9417371 and PHY-9424337 and by NASA grant NAGW-4268/NAG5-4351. Large portions of this article were adapted and updated from my Ref. [105].

References

- [1] J. Weber. *Phys. Rev.*, 117:306, 1960.
- [2] R. Weiss. *Quarterly Progress Report of RLE, MIT*, 105:54, 1972.
- [3] M. S. Turner. *Phys. Rev. D*, 55:R435, 1997.
- [4] L. P. Grishchuk. *Phys. Rev. D*, 53:6784, 1996.
- [5] M. Gasperini, M. Giovannini, and G. Veneziano. *Phys. Rev. D*, 52:R6651, 1995.
- [6] V. M. Kaspi, J. H. Taylor, and M. F. Ryba. *Astrophys. J.*, 428:713, 1994.
- [7] Ya. B. Zel'dovich. *Mon. Not. Roy. Astron. Soc.*, 192:663, 1980.
- [8] A. Vilenkin. *Phys. Rev. D*, 24:2082, 1981.
- [9] A. Kosowsky and M. S. Turner. *Phys. Rev. D*, 49:2837, 1994.
- [10] X. Martin and A. Vilenkin. *Phys. Rev. Lett.*, 77:2879, 1996.
- [11] K. S. Thorne. In S. W. Hawking and W. Israel, editors, *Three Hundred Years of Gravitation*, pages 330–458. Cambridge University Press, 1987.
- [12] A. Abramovici et. al. *Science*, 256:325, 1992.
- [13] A. Abramovici et. al. *Physics Letters A*, 218:157, 1996.
- [14] C. Bradaschia et. al. *Nucl. Instrum. & Methods*, A289:518, 1990.
- [15] B. Barish and G. Sanders et. al. LIGO Advanced R and D Program Proposal, Caltech/MIT, unpublished, 1996.
- [16] J. Hough and K. Danzmann et. al. GEO600, Proposal for a 600 m Laser-Interferometric Gravitational Wave Antenna, unpublished, 1994.
- [17] K. Kuroda et. al. In I. Ciufolini and F. Fiducaro, editors, *Gravitational Waves: Sources and Detectors*, page 100. World Scientific, 1997.
- [18] B. J. Meers. *Phys. Rev. D*, 38:2317, 1988.
- [19] M. J. Mizuno, K. A. Strain, P. G. Nelson, J. M. Chen, R. Schilling, A. Rudiger, W. Winkler, and K. Danzman. *Phys. Lett. A*, 175:273, 1993.
- [20] W. W. Johnson and S. M. Merkowitz. *Phys. Rev. Lett.*, 70:2367, 1993.
- [21] G. Frossati. *J. Low Temp. Phys.*, 101:81, 1995.
- [22] G. V. Pallottino. In I. Ciufolini and F. Fiducaro, editors, *Gravitational Waves: Sources and Detectors*, page 159. World Scientific, 1997.
- [23] P. Bender et. al. *LISA, Laser interferometer space antenna for the detection and observation of gravitational waves: Pre-Phase A Report*. Max-Planck-Institut für Quantenoptik, MPQ 208, December 1995.

- [24] A. G. Petschek, editor. *Supernovae*. Springer Verlag, 1990.
- [25] H. A. Bethe. *Rev. Mod. Phys*, 62:801, 1990.
- [26] A. Burrows, 1994. Private communication.
- [27] E. Müller and H.-T. Janka. *Astron. Astrophys.*, 317:140, 1997.
- [28] L. S. Finn. *Ann. N. Y. Acad. Sci.*, 631:156, 1991.
- [29] R. Mönchmeyer, G. Schäfer, E. Müller, and R. E. Kates. *Astron. Astrophys.*, 256:417, 1991.
- [30] B. F. Schutz. *Class. Quant. Grav.*, 6:1761, 1989.
- [31] D. Lai and S. L. Shapiro. *Astrophys. J.*, 442:259, 1995.
- [32] J. L. Houser, J. M. Centrella, and S. C. Smith. *Phys. Rev. Lett.*, 72:1314, 1994.
- [33] I. A. Bonnell and J. E. Pringle. *Mon. Not. Roy. Astron. Soc.*, 273:L12, 1995.
- [34] M. Zimmermann and E. Szedenits. *Phys. Rev. D*, 20:351, 1979.
- [35] S. L. Shapiro and S. A. Teukolsky. Wiley: Interscience, 1983. Section 10.10 and references cited therein.
- [36] P. Brady, T. Creighton, C. Cutler, and B. Schutz. *Phys. Rev. D*, 1997. Submitted; gr-qc/9702050.
- [37] B. F. Schutz, 1995. Private communication.
- [38] S. Chandrasekhar. *Phys. Rev. Lett.*, 24:611, 1970.
- [39] J. L. Friedman and B. F. Schutz. *Astrophys. J.*, 222:281, 1978.
- [40] R. V. Wagoner. *Astrophys. J.*, 278:345, 1984.
- [41] L. Lindblom. *Astrophys. J.*, 438:265, 1995.
- [42] L. Lindblom and G. Mendell. *Astrophys. J.*, 444:804, 1995.
- [43] R. A. Hulse and J. H. Taylor. *Astrophys. J.*, 324:355, 1975.
- [44] J. H. Taylor. *Rev. Mod. Phys.*, 66:711, 1994.
- [45] R. Narayan, T. Piran, and A. Shemi. *Astrophys. J.*, 379:L17, 1991.
- [46] E. S. Phinney. *Astrophys. J.*, 380:L17, 1991.
- [47] E. P. J. van den Heuvel and D. R. Lorimer. *Mon. Not. Roy. Astron. Soc.*, 1996. In press.
- [48] A. V. Tutukov and L. R. Yungelson. *Mon. Not. Roy. Astron. Soc.*, 260:675, 1993.
- [49] H. Yamaoka, T. Shigeyama, and K. Nomoto. *Astron. Astrophys.*, 267:433, 1993.

- [50] V. M. Lipunov, K. A. Postnov, and M. E. Prokhorov. *Astrophys. J.*, 423:L121, 1994. And related, unpublished work.
- [51] V. M. Lipunov, K. A. Postnov, and M. E. Prokhorov. *Astrophys. J.* Submitted; astro-ph/9610016.
- [52] S. F. P. Zwart and H. N. Spreeuw. *Astron. Astrophys.*, 312:670, 1996.
- [53] D. Hils, P. Bender, and R. F. Webbink. *Astrophys. J.*, 360:75, 1990.
- [54] C. Cutler. *Phys. Rev. D*, 1995. Submitted; gr/qc-9703068.
- [55] C. Kochanek. *Astrophys. J.*, 398:234, 1992.
- [56] L. Bildsten and C. Cutler. *Astrophys. J.*, 400:175, 1992.
- [57] G. Quinlan and S. L. Shapiro. *Astrophys. J.*, 321:199, 1987.
- [58] B. F. Schutz. *Nature*, 323:310, 1986.
- [59] C. Cutler, T. A. Apostolatos, L. Bildsten, L. S. Finn, E. E. Flanagan, D. Kennefick, D. M. Markovic, A. Ori, E. Poisson, G. J. Sussman, and K. S. Thorne. *Phys. Rev. Lett.*, 70:1984, 1993.
- [60] C. M. Will. In M. Sasaki, editor, *Relativistic Cosmology*, page 83. Universal Academy Press, 1994.
- [61] T. A. Apostolatos, C. Cutler, G. J. Sussman, and K. S. Thorne. *Phys. Rev. D*, 49:6274, 1994.
- [62] L. E. Kidder. *Phys. Rev. D*, 52:821, 1995.
- [63] C. Cutler and E. E. Flanagan. *Phys. Rev. D*, 49:2658, 1994.
- [64] L. S. Finn and D. F. Chernoff. *Phys. Rev. D*, 47:2198, 1993.
- [65] E. Poisson and C. M. Will. *Phys. Rev. D*, 52:848, 1995.
- [66] L. Blanchet, T. Damour, B. R. Iyer, C. M. Will, and A. G. Wiseman. *Phys. Rev. Lett.*, 74:3515, 1995.
- [67] S. Chandrasekhar. *Selected Papers of S. Chandrasekhar, Vol. 5, Relativistic Astrophysics*. U. Chicago Press, 1990.
- [68] S. Chandrasekhar and F. P. Esposito. *Astrophys. J.*, 160:153, 1970.
- [69] C. Cutler and E. E. Flanagan. *Phys. Rev. D*. Paper in preparation.
- [70] T. Damour and B.S. Sathyaprakash. Research in progress, 1997.
- [71] B. J. Owen. *Phys. Rev. D*, 53:6749, 1996.
- [72] S. A. Hughes, D. Kennefick, D. Laurence, and K. S. Thorne. *Phys. Rev. D*. In preparation.

- [73] Z. G. Xing, J. M. Centrella, and S. L. W. McMillan. *Phys. Rev. D*, 54:7261, 1996. Also references therein.
- [74] M. R. Metzger et. al. *Nature*. Submitted.
- [75] P. Meszaros. *Ann. N.Y. Acad. Sci.*, 759:440, 1995.
- [76] S. E. Woosley. *Ann. N.Y. Acad. Sci.*, 759:446, 1995.
- [77] E. E. Flanagan and S. A. Hughes. *Phys. Rev. D*, 1997. Submitted; gr/qc-9701039.
- [78] Numerical Relativity Grand Challenge Alliance, 1995. References and information on the World Wide Web, <http://jean-luc.ncsa.uiuc.edu/GC>.
- [79] S. Chandrasekhar and S. L. Detweiler. *Proc. Roy. Soc. A*, 344:441, 1975.
- [80] S. L. Detweiler. *Astrophys. J.*, 239:292, 1980.
- [81] S. Chandrasekhar. *The Mathematical Theory of Black Holes*. Oxford University Press, 1983.
- [82] E. W. Kolb and M. S. Turner. *The Early Universe*. Addison-Wesley, 1990. Pages 40–43.
- [83] M. G. Haehnelt. *Mon. Not. Roy. Astron. Soc.*, 269:199, 1994.
- [84] D. Christodoulou. *Phys. Rev. Lett.*, 67:1486, 1991.
- [85] K. S. Thorne. *Phys. Rev. D*, 45:520–524, 1992.
- [86] A. G. Wiseman and C. M. Will. *Phys. Rev. D*, 44:R2945, 1991.
- [87] D. Kennefick. *Phys. Rev. D*, 50:3587, 1994.
- [88] T. Damour and K. Nordtvedt. *Phys. Rev. D*, 48:3436, 1993.
- [89] C. M. Will. *Phys. Rev. D*, 50:6058, 1994.
- [90] D. Markovic. *Phys. Rev. D*, 48:4738, 1993.
- [91] D. F. Chernoff and L. S. Finn. *Astrophys. J. Lett.*, 411:L5, 1993.
- [92] F. D. Ryan. *Phys. Rev. D*, 52:5707, 1995.
- [93] F. D. Ryan. Accuracy of estimating the multipole moments of a massive body from the gravitational waves of a binary inspiral. *Phys. Rev. D*, 1997. Submitted.
- [94] L. S. Finn and K. S. Thorne. *Phys. Rev. D*. In preparation.
- [95] F. D. Ryan. Spinning boson stars with large self-interaction. *Phys. Rev. D*, 1997. In press.
- [96] T. D. Lee and Y. Pang. *Physics Reports*, 221:251, 1992.
- [97] S. K. Chakrabarti. *Phys. Rev. D*, 53:2901, 1996.
- [98] F. D. Ryan, L. S. Finn, and K. S. Thorne. *Phys. Rev. Lett.* In preparation.

- [99] D. Hils and P. Bender. *Astrophys. J. Lett*, 445:L7, 1995.
- [100] S. Sigurdsson and M. J. Rees. *Mon. Not. Roy. Astron. Soc.*, 284:318, 1997.
- [101] F. D. Ryan. Scalar waves produced by a scalar charge orbiting a massive body with arbitrary multipole moments. *Phys. Rev. D*, 1997. Submitted.
- [102] Y. Mino, M. Sasaki, and T. Tanaka. *Phys. Rev. D*, 55:3497, 1997.
- [103] T. C. Quinn and R. M. Wald. *Phys. Rev. D*. Submitted; gr-qc/9610053.
- [104] G. E. Moss, L. R. Miller, and R. L. Forward. *Applied Optics*, 10:2495, 1971.
- [105] K. S. Thorne. In E. W. Kolb and R. Peccei, editors, *Proceedings of the Snowmass 95 Summer Study on Particle and Nuclear Astrophysics and Cosmology*, page 398. World Scientific, 1995.